Supplemental materials for EHP ms 11771:

Developmental Exposure to Polychlorinated Biphenyls Interferes with Experience-Dependent Dendritic Plasticity and Ryanodine Receptor Expression in Weanling Rats

Dongren Yang[1*], Kyung Ho Kim[2*], Andrew Phimister[2], Adam D. Bachstetter[3], Thomas R. Ward[4], Robert W. Stackman[5], Ronald F. Mervis[3], Amy B. Wisniewski[6], Sabra L. Klein[7], Prasada Rao S. Kodavanti[4], Kim A. Anderson[8], Gary Wayman[9], Isaac N. Pessah[2], Pamela J. Lein[1,10]

[1]Center for Research on Occupational and Environmental Toxicology, Oregon Health & Science University, Portland, OR, USA; [2]Veterinary Molecular Biosciences and Center for Children's Environmental Health, University of California, Davis, CA, USA; [3]Neurostructural Research Labs and Center for Aging and Brain Repair, University of South Florida College of Medicine, Tampa, FL, USA; [4]Neurotoxicology Division, National Health and Environmental Effects Research Laboratory, ORD, USEPA, Research Triangle Park, NC, USA; [5]Psychology, Florida Atlantic University, Boca Raton, FL, USA; [6]Pediatrics, University of Oklahoma Health Sciences Center, Oklahoma City, OK, USA; [7]Molecular Microbiology and Immunology, Johns Hopkins University Bloomberg School of Public Health, Baltimore, MD, USA; [8]Environmental & Molecular Toxicology, Oregon State University, Corvallis, OR; USA; [9]Veterinary and Comparative Anatomy, Physiology and Pharmacology, Washington State University, Pullman, WA, USA; [10]Environmental Health Science, Johns Hopkins University Bloomberg School of Public Health, Baltimore, MD, USA. *These authors contributed equally to this work.

Corresponding author: Pamela J. Lein, Ph.D.
Oregon Health & Science University, CROET/L606
3181 SW Sam Jackson Park Road, Portland, OR 97239
Email: leinp@ohsu.edu;
Phone: 503-494-9279
Fax: 503-494-3849

Materials and Methods

Morris water maze. At P24, spatial learning and memory was assessed in one male and one female rat from 11 different litters within each treatment group using the Morris water maze (Morris 1984) as previously described (Jett et al. 1997). Details are provided in supplemental online material. Testing was conducted in a round white pool (0.9m in diameter and 0.5m deep) in a room containing several visual cues that remained in a fixed position around the room throughout the testing period. The pool was filled to a depth of 30cm with water made opaque with white, certified nontoxic water-based tempura paint. Water temperature was maintained at 20±2°C. The escape platform, a 25cm^2 Plexiglas disc hidden 1–3cm below the surface of water, was placed in the middle of one quadrant of the pool, 15cm from the edge. A trial began by placing the rat on the platform for 20s to allow it to orient to visual cues in the room. The rat was then randomly placed in the pool facing the wall in 1 of 12 positions delineated as hour positions on a clock and allowed to swim to the hidden platform. The escape latency (time required to find the hidden platform) and distance traveled were automatically recorded using a digital tracking system (Videomex-V Image Analyzer, Columbus Instruments, Columbus, OH). Each rat was given 45s to find the hidden platform. Previous experiments indicated that weanling rats do not fatigue in this time period (Jett et al. 2001). If the platform was not found within 45s, the rat was gently guided to the platform. All rats were allowed to sit on the platform for an additional 20s after the completion of the trial before being placed in drying cages in front of portable heaters to facilitate drying and prevent hypothermia. These heaters also provided white noise during the trials. Behavioral testing was conducted daily between 0900 and 1100h for 7d. Rats were tested in one trial per day, except on the first day, when two trials were administered. This modification of the swim task increases the difficulty of the task, such that relatively small differences

between treatment groups can be detected, yet the task is not too difficult for rats to learn quickly (Jett et al. 1997; Jett et al. 2001; Kuhlmann et al. 1997).

An escape latency of 10s was chosen as the criterion to indicate that animals had learned the task based on previous studies using rats of comparable age in a similar size test pool (Jett et al. 1997; Jett et al. 2001; Markwiese et al. 1998; Rudy et al. 1987). To test spatial memory, a probe test was administered 30min after the spatial training trials on the first day that the mean escape latency of control- and A1254-animals reached their respective criterion. In this test, the platform was removed from the pool and rats were allowed to swim freely for 45s. Computer software was programmed to record the distance traveled and the time spent in each quadrant of the pool, and the magnitude of spatial memory retention was determined by the amount of time spent in the quadrant where the platform had been positioned during learning trials. A visual cue test was conducted immediately following the probe test to determine whether performance was impacted by visual, motor or motivational deficits (McNamara and Skelton 1993). In this test, the platform position was marked with a black flag so that rats could readily locate the platform using a local visual stimulus. The parameters measured included escape latency, path length and swimming speed.

Morphometric analyses of dendritic arborization. Upon completion of the Morris water maze tests on P31, animals were euthanized and perfused with 4% paraformaldehyde. To visualize dendritic arbors of Purkinje cells, parasagittal cryosections (12μm thick) cut from both hemispheres of the cerebellum starting 1mm from the midline were immunostained for calbindin-D_{28K} (anti-calbindin-D_{28K} antibody was purchased from Sigma), which has been shown to specifically label Purkinje cells within the cerebellum (Christakos et al. 1987; Wassef et al. 1985). Sections were coded so that individuals doing the morphometric analyses were blinded to

treatment conditions. The criteria used to select individual neurons for analysis included: 1) localized to the cerebellar vermis; 2) planar dendritic arbor largely parallel to the focal plane; 3) dendritic arbors fully stained and not obscured by neighboring cells; and 4) dendritic tree intact with no cut dendritic segments. Digital images of individual neurons were captured using a Spot cooled CCD camera and Spot image acquisition software (Diagnostic Imaging, Sterling, MI) interfaced to a Nikon E400 microscope equipped for epifluorescence. The total length of the dendritic arbor was quantified using Metamorph imaging software (v1.62, Molecular Devices, Sunnyvale, CA).

Dendritic arbors of neocortical neurons were visualized by Golgi staining. Coronal blocks from approximately Bregma -1.06 to -2.80mm that included the parietal cortex were stained using the Rapid Golgi protocol (Valverde 1993), embedded in nitrocellulose and the tissue block then sectioned at a thickness of 120μm. Dendritic length was quantified from camera lucida drawings of the soma and basilar dendritic arbor of 6-7 pyramidal neurons from neocortical layer V randomly selected from each of 5 brains per treatment group by individuals blinded to the treatment. Study inclusion criteria included: 1) neuron well-impregnated with no evidence of incomplete or artificial staining; 2) neuron and dendritic branches not obscured by blood vessels, glia, or non-descript precipitate; 3) cell body located in the middle third of the thickness of the section to eliminate bias based on the size of the dendritic arbor; and 4) neuron located along the dorsal convexity of the cerebrum extending laterally from the rhinal fissure up to, but not including, the cingulate gyrus (medially). The dendritic arbor was quantified by Sholl Analysis (Sholl 1953; Uylings and van Pelt 2002), a method in which the number of dendritic branches intersecting concentric circles of 10μm increments centered on the soma is determined. This analysis defines the amount and distribution of the dendritic arbor at increasing distances

from the cell body, and the total number of intersections per neuron provides an estimate of the total dendritic length of the basilar dendritic tree.

Dendritic arbors were visualized in dissociated cultures of neocortical neurons transfected with plasmid encoding a microtubule-associated protein-2 (MAP2)-enhanced green fluorescent protein (GFP) fusion construct prior to experimental exposures, then fixed in 4% paraformaldehyde and immunostained for GFP immediately following experimental exposures, as previously described (Wayman et al. 2006). Digital images of GFP immunopositive neurons were recorded using a SPOT cooled CCD camera and total dendritic length determined using SPOT imaging software (Diagnostic Imaging). An average of 10 neurons per culture from 3 cultures per treatment group was analyzed, and data were confirmed in two independent dissections.

RyR profiling. Specific [^{3}H]ryanodine (5nM) binding to whole particulate cerebellar membranes isolated from control and A1254 treatment groups was measured at P21 and P31, as previously described (Wong et al. 1997). For P21 samples, a [^{3}H]ryanodine binding curve (0.625-5nM) was also measured. Binding constants (K_d, B_{max}) were determined by Scatchard plot analysis. To profile RyR expression, protein in whole membrane fractions were size-separated on 4-15% gradient SDS-PAGE gels under denaturing conditions, transferred onto PVDF membranes, immunoblotted with antibody 34C specific for RyR1/3 subtypes (Univ. Iowa Hybridoma Bank, culture media) or antibody C3-33 specific for RyR2 subtype (Alexis Biochemicals, San Diego, CA). Immunoblots were visualized by enhanced chemiluminescence (ECL, Pierce) and quantified by densitometry as previously described (Roegge et al. 2006). Density values were determined from at least 4 blots.

Congener-specific PCB analyses. Whole brains harvested from P31 rats were stored at -80°C and thawed immediately before extraction, cleanup, and fractionation using gel permeation chromatography as previously described (Sethajintanin et al. 2004). Tetrachloro-m-xylene in hexanes was used in all samples as the internal surrogate standard. Additional fortification samples spiked with a 20-ng/g PCB mixture were included in all batches. Specific PCB congeners were determined using gas chromatography coupled to micro-electrochemical detection (GC-μECD, Agilent Technologies 6890N Network GC system) as previously described (Sethajintanin and Anderson 2006). To minimize batch-to-batch bias, samples from any designated group were typically analyzed in three different batches. Reagent and extraction blanks were included in every batch. Quality control samples represented 30-40% of a sample set and were processed and analyzed exactly the same as samples. The method detection limits were determined as 3 times the heights of coincident peaks observed for each compound in the control rat tissue. None of the target analytes were identified in the reagent or extraction blanks. Recovery of the internal surrogate ranged from 45-86%. The average percent recovery of fortified samples was 60-97% for target congeners.

Statistical analyses. Behavioral data were analyzed using repeated measures ANOVA with gender and treatment as main effects and trial day as the repeated measure and treatment effects on each trial day were evaluated using Newman-Keuls Multiple Comparison Test. Sholl data were evaluated using the Wilcoxon rank-sign test applying a highly conservative alpha level based on the number of measurements (Dawson and Trapp 2004). All other data were analyzed by unpaired Fisher's exact test, T-tests or ANOVA ($p<0.05$) as indicated in the figure legends. *Post-hoc* mean comparisons were performed using the Newman-Keuls Multiple Comparison Test unless otherwise noted.

References

Christakos S, Rhoten WB, Feldman SC. 1987. Rat calbindin D28K: purification, quantitation, immunocytochemical localization, and comparative aspects. Methods in enzymology 139:534-551.

Dawson B, Trapp RG. 2004. Basic and Clinical Biostatistics. 4th ed. New York: Lange Medical Books.

Jett DA, Kuhlmann AC, Farmer SJ, Guilarte TR. 1997. Age-dependent effects of developmental lead exposure on performance in the Morris water maze. Pharmacol Biochem Behav 57(1-2):271-279.

Jett DA, Navoa RV, Beckles RA, McLemore GL. 2001. Cognitive function and cholinergic neurochemistry in weanling rats exposed to chlorpyrifos. Toxicol Appl Pharmacol 174(2):89-98.

Kuhlmann AC, McGlothan JL, Guilarte TR. 1997. Developmental lead exposure causes spatial learning deficits in adult rats. Neuroscience letters 233(2-3):101-104.

Markwiese BJ, Acheson SK, Levin ED, Wilson WA, Swartzwelder HS. 1998. Differential effects of ethanol on memory in adolescent and adult rats. Alcoholism, clinical and experimental research 22(2):416-421.

McNamara RK, Skelton RW. 1993. The neuropharmacological and neurochemical basis of place learning in the Morris water maze. Brain Res Brain Res Rev 18(1):33-49.

Morris R. 1984. Developments of a water-maze procedure for studying spatial learning in the rat. J Neurosci Methods 11(1):47-60.

Roegge CS, Morris JR, Villareal S, Wang VC, Powers BE, Klintsova AY, et al. 2006. Purkinje cell and cerebellar effects following developmental exposure to PCBs and/or MeHg. Neurotoxicol Teratol 28(1):74-85.

Rudy JW, Stadler-Morris S, Albert P. 1987. Ontogeny of spatial navigation behaviors in the rat: dissociation of "proximal"- and "distal"-cue-based behaviors. Behav Neurosci 101(1):62-73.

Sethajintanin D, Johnson ER, Loper BR, Anderson KA. 2004. Bioaccumulation profiles of chemical contaminants in fish from the lower Willamette River, Portland Harbor, Oregon. Archives of environmental contamination and toxicology 46(1):114-123.

Sethajintanin D, Anderson KA. 2006. Temporal bioavailability of organochlorine pesticides and PCBs. Environ Sci Technol 40(12):3689-3695.

Sholl DA. 1953. Dendritic organization in the neurons of the visual and motor cortices of the cat. J Anat 87(4):387-406.

Uylings HB, van Pelt J. 2002. Measures for quantifying dendritic arborizations. Network (Bristol, England) 13(3):397-414.

Valverde F. 1993. The rapid Golgi technique for staining CNS neurons: Light microscopy. Neuroscience Protocols 1:1-9.

Wassef M, Zanetta JP, Brehier A, Sotelo C. 1985. Transient biochemical compartmentalization of Purkinje cells during early cerebellar development. Developmental biology 111(1):129-137.

Wayman GA, Impey S, Marks D, Saneyoshi T, Grant WF, Derkach V, et al. 2006. Activity-dependent dendritic arborization mediated by CaM-kinase I activation and enhanced CREB-dependent transcription of Wnt-2. Neuron 50(6):897-909.

Wong PW, Brackney WR, Pessah IN. 1997. Ortho-substituted polychlorinated biphenyls alter microsomal calcium transport by direct interaction with ryanodine receptors of mammalian brain. J Biol Chem 272(24):15145-15153.

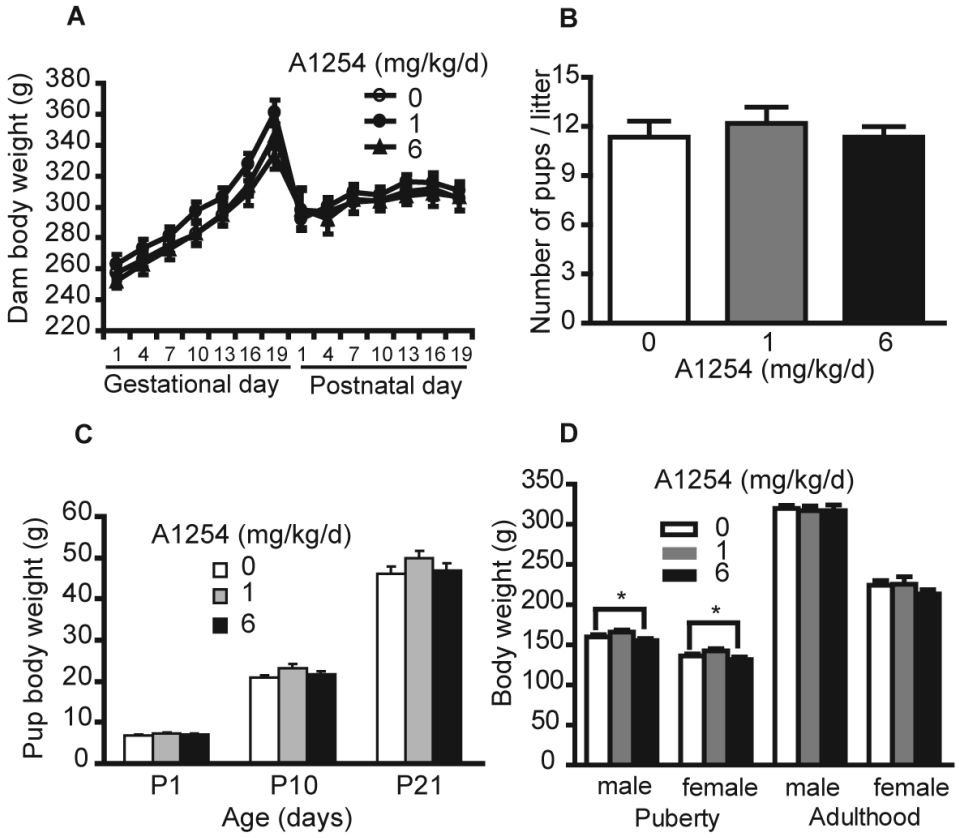

Supplemental Figure 1. Developmental A1254 exposure does not cause maternal or fetal toxicity. Exposure to A1254 in the maternal diet throughout gestation and lactation did not alter: (A) the body weight of pregnant and lactating dams (N≥10 per group), (B) litter size or (C) growth rates of the pups during early development stages (N≥100 per group). (D) Exposure to 6 mg/kg/d A1254 in the maternal diet caused a transient decrease in weight at puberty (P40, N≥30 per treatment group) that did not persist into adulthood (P70, N≥15 per group). Data presented as the mean±SEM; *$p<0.05$ (all data were analyzed using repeated measures ANOVA except the number of pups/litter which was analyzed using one-way ANOVA with *post hoc* Newman-Keuls Multiple Comparison Test).

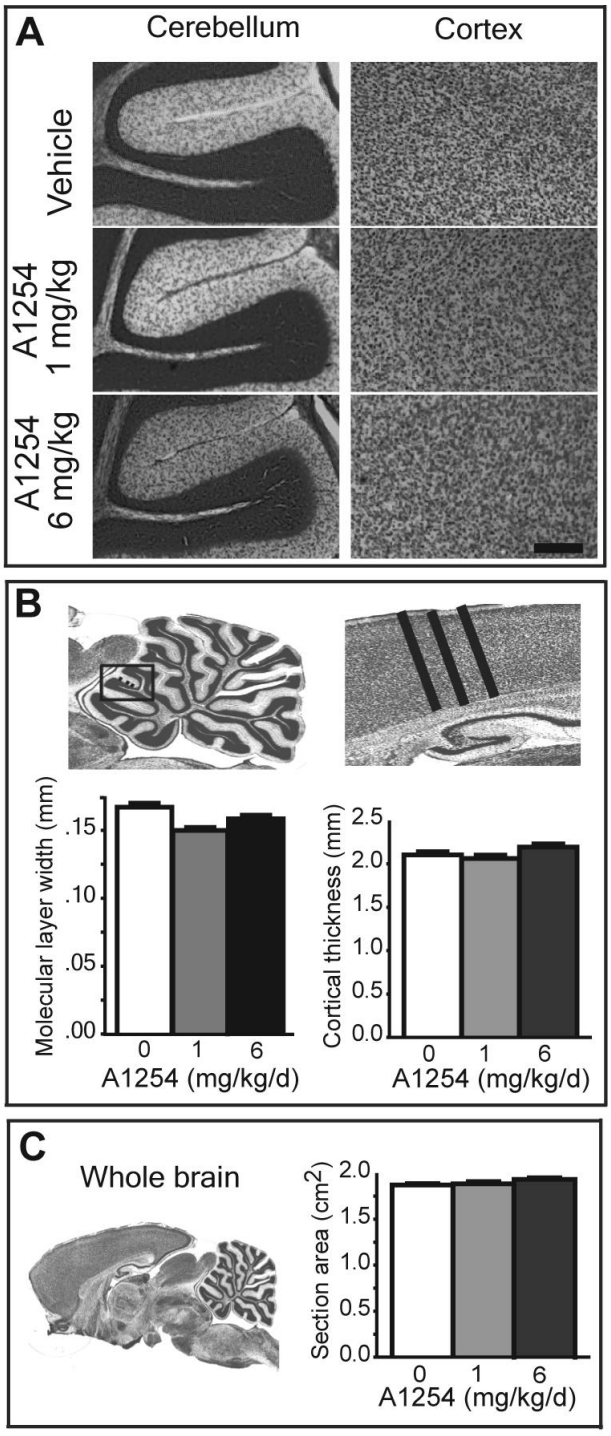

Supplemental Figure 2. Developmental A1254 exposure does not cause gross histological changes in the cerebellum or neocortex at P31. (A) Nissl staining of serial sagittal sections of

fixed brain (50μm thick, 5-6 sections per rat, 5 rats per group) obtained approximately 1mm from the midline indicated no obvious treatment-related histological changes in either the cerebellum (left) or neocortex (right). (B) Developmental A1254 exposure had no effect on molecular layer widths in cerebellar lobule 3 (left) or on cortical thickness between layer I and the beginning of the white matter beneath layer VI in the cerebral neocortex (right). For each section, three measurements of comparable areas within each brain region were obtained. (C) The overall size of brains as determined by cross-sectional area of sections. Data represented as the mean±SEM (n=25-30 sections; 5 brains per experimental group). Statistical significance was evaluated using one-way ANOVA followed by Newman-Keuls Multiple Comparison Test. Scale bar = 200μm